Journal of
Mechanics of
Materials and Structures

MIXED PIEZOELECTRIC PLATE ELEMENTS WITH CONTINUOUS TRANSVERSE ELECTRIC DISPLACEMENTS

Erasmo Carrera and Christian Fagiano

Volume 2, Nº 3 March 2007

mathematical sciences publishers

JOURNAL OF MECHANICS OF MATERIALS AND STRUCTURES
Vol. 2, No. 3, 2007

MIXED PIEZOELECTRIC PLATE ELEMENTS WITH CONTINUOUS TRANSVERSE ELECTRIC DISPLACEMENTS

ERASMO CARRERA AND CHRISTIAN FAGIANO

This paper proposes mixed finite elements, FEs, with an *a priori* continuous transverse electric displacement component $\mathcal{D}_z$. The Reissner Mixed Variational Theorem (RMVT) and the Unified Formulation (UF) are applied to the analysis of multilayered anisotropic plates with embedded piezoelectric layers. Two forms of RMVT are compared. In a first, *partial*, form (P-RMVT), the field variables are displacements $\boldsymbol{u}$, electric potential Φ and transverse stresses $\boldsymbol{\sigma}_n$. The second, *full*, form (F-RMVT) adds $\mathcal{D}_z$ as an independent variable. F-RMVT allows the *a priori* and complete fulfillment of interlaminar continuity of both mechanical and electrical variables.

We treat both equivalent single-layer models (ESLM), where the number of variables is kept independent of the number of layers, an layerwise models (LWM), in which the number of variables depends in each layer. According to the UF the order N of the expansions assumed for the $\boldsymbol{u}$, ϕ, $\boldsymbol{\sigma}_n$ and $\mathcal{D}_z$ fields in the plate thickness direction z as well as the number of the element nodes N_n have been taken as free parameters.

In most cases the results of the classical formulation which are based on Principle of Virtual Displacements (PVD) are given for comparison purposes. The superiority of the F-RMVT results, with respect to the P-RMVT and to PVD ones, is shown by few examples for which three-dimensional solution is available. In particular, the F-RMVT results to be very effective for the evaluation of interlaminar continuous $\mathcal{D}_z$ fields.

1. Introduction

In recent years piezoelectric materials have been integrated with structural systems to build smart structures which are the candidates for next generation structures of aerospace vehicles as well as for some advanced products in the automotive and ship industries. Piezoelectric materials are, in fact, capable of altering the response of the structures through sensing and actuation [Tiersten 1969]. By integrating the surface bonded and embedded actuators in structural systems, the desired localized strains may be induced in the structures thanks to the application of an appropriate voltage to the actuators. Such an electromechanical coupling allows closed-loop control systems to be built up, in which piezomaterials play the role of both the actuators and the sensors. An intelligent structure can therefore be built in which, for instance, thermomechanical deformations or vibrations can be reduced by using appropriate control laws. For details see [Chopra 1996; 2002] and the related literature.

In order to successfully incorporate actuator/sensors in a structures, the mechanical interaction between the piezoelectric layers and the hosting structure must be completely understood, that is, an

Keywords: piezoelectric plates, finite elements, mixed method, transverse continuity, unified formulation.
This work has been carried out in the framework of STREP EU project CASSEM under contract NMP-CT-2005-013517.

appropriate use of piezoelectric materials, requires an accurate description of both the electrical and mechanical fields in the constitutive layers. Early mechanical models were developed by Crawley and de Luis [1987], Lee [1990] and Mitchell and Reddy [1995], among others. More recent works are [Yang and Batra 1995; Wang et al. 1997; Vidoli and Batra 2000; Batra and Vidoli 2002]. A recent assessment of classical and refined theories with displacements and electrical variables for plates can be found in [Ballhause et al. 2005]. Equivalent single-layer (ESL) and layerwise (LW) theories have been compared in the framework of the application of the Principle of Virtual Displacement (PVD) applications (it is intended that the number of independent variables is kept independent by the number of the layers in the ESL models). Numerous benchmark, exact solution analyses have been conduced for piezoelectric plates; some are given in [Heyliger and Saravanos 1995]. However, these benchmark solutions are restricted to simple geometries and special boundary conditions. The treatment of more realistic problems would require the use of efficient computational tools such as the finite element method (FEM).

The present paper focuses on FEM electromechanical two-dimensional modelings of smart structures with embedded piezo layers. Finite element studies were conducted by Robbins and Reddy [1991]. A finite element that accounts for a first order shear deformation theory (FSDT) description of displacement and layerwise form of the electric potential was developed in [Sheikh et al. 2001]. The numerical, membrane and bending behavior of the FEs based on FSDT was analyzed in [Auricchio et al. 2001] in the framework of a suitable variational formulation. The third-order theory was applied by Thornbuegh and Chattopadhyay [2002] to derived finite elements that account for electromechanical coupling. Similar elements have more recently been considered in [Shu 2005]. Extension of the third-order Ambartsumian zigzag multilayered theory [Carrera 2003a] to the finite analysis of electromechanical problems has been proposed by Oh and Cho [2004]. An extension of numerically efficient plate/shell elements based on mixed interpolation of tensorial components (MITC) to piezoelectric plates has recently been provided by Kögl and Bucalem [2005a; 2005b]. We also mention the review papers [Saravanos and Heyliger 1999; Benjeddou 2000; Wang and Yang 2000].

Our contributions to the application of the Reissner Mixed Variational Theorem (RMVT) to multilayered made structures started with [Carrera 1995; 1996; 2001], and have included closed-form solution analyses [Carrera 1999a; 1999b] and FE applications [Carrera and DeMasi 2002a; 2002b], showing the RMVT is a very suitable tool to provide quasi-3D description of stress and strain fields in anisotropic laminated structures. The RMVT was also employed in the framework of Unified Formulation (UF), dealt with in detail in [Carrera 2001]. The main feature of UF is that it allows one to formulate both ESLM and LW models in terms of a few fundamental nuclei whose forms do not depend on either the order of the expansion N used for the various variables (in the thickness direction) or on by the number of nodes of the element N_n. The Murakami zigzag Function (MZZF) [Carrera 2001] was used to reproduce the zigzag form of displacement field in the ESLM case. A classical formulation, based on PVD, was developed for comparison purposes.

A first application of RMVT to piezoelectric plates was provided in [Carrera 1997], where an MITC-type plate element was extended to nonlinear dynamic analysis of piezoelectric, composite plate. The UF formulation was applied, in the PVD framework, to piezoelectric plates in [Ballhause et al. 2005]; attention was restricted to analytical closed form solutions. RMVT closed form solutions were presented in [D'Ottavio and Kröplin 2006], while extension to shell has been provided in [Carrera et al. 2005]. Finite element applications have also been provided recently [Carrera and Boscolo 2006].

All these RMVT works have been restricted to the *a priori* fulfillment of the interlaminar continuity of the mechanical variables (transverse normal and shear stress fields), that is, the continuity of transverse normal component $\mathcal{D}_z$ of the electric displacement vector was not *a priori* guaranteed. This form of RMVT is herein referred to as the *partial* form, or P-RMVT. RMVT has also been applied in [Garcia Lage et al. 2004a] to develop LW piezoelectric plate elements in the static case. The transverse component of electric displacement $\mathcal{D}_z$ was considered as an assumed variable. We refer to such an extension as *full* RMVT applications, namely F-RMVT. Garcia Lage and his coauthors restricted their attention to the quadratic distribution of displacements (mechanical and electrical) and transverse stress unknowns, and treated only a layerwise model. These restrictions have not allowed us to analyze the features of the *a priori* assumption of interlaminar continuous transverse electric displacement.

Here we compares P-RMVT and F-RMVT in the framework of UF, extending the analysis of [Carrera and Boscolo 2006] to include the normal electrical displacement $\mathcal{D}_z$ as an assumed *a priori* variable. A number of new finite elements are derived and systematically compared to those based on P-RMVT and PVD. ESLM and LW variable description analyses are compared to available 3D solutions. Up to forth-order expansions in the thickness plate/layers have been implemented.

The paper is organized as follows. Section 2 gives the necessary preliminaries. Section 3 introduces the two RMVT forms for piezoelectric continua along with variationally consistent constitutive equations. The UF for finite element applications are derived in Section 3, and the FE matrices themselves in Section 5. Section 6 contains numerical results and discussion.

2. Preliminaries

Figure 1 shows the geometry and the coordinate system of a laminated plate with N_l layers, including piezoelectric layers. The reference system is denoted by x, y, z; the correspondent plate dimensions are denoted by a, b, h, the last of which is the thickness.

The material properties of a piezoelectric continuum can be expressed in different forms; we use the so-called e-form [Ikeda 1996]. The relevant energy is then the electric Gibbs energy G_2, which takes the form

$$G_2 = \tfrac{1}{2}\boldsymbol{\epsilon}^T \boldsymbol{C}^{\mathscr{E}} \boldsymbol{\epsilon} - \mathscr{E}^T \boldsymbol{e}\boldsymbol{\epsilon} - \tfrac{1}{2}\mathscr{E}^T \boldsymbol{\varepsilon}^{\epsilon} \mathscr{E}, \tag{1}$$

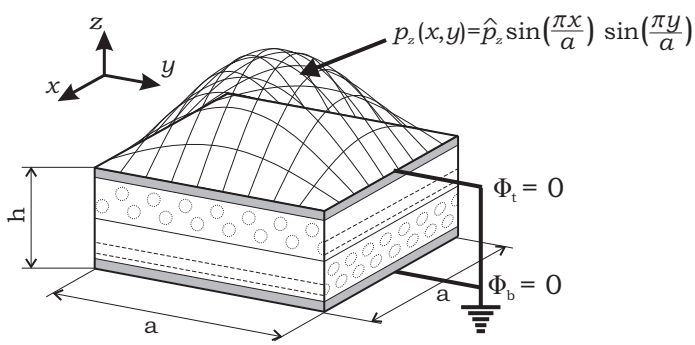

Figure 1. Geometry of Piezoelectric Plate

where $\boldsymbol{\epsilon}^T = \{\epsilon_{xx}, \epsilon_{yy}, \epsilon_{zz}, \epsilon_{xz}, \epsilon_{yz}, \epsilon_{xy}\}$ is the strain tensor (we use bold letters for arrays and T to denote transposition), $\mathscr{E}^T = \{\mathscr{E}_x, \mathscr{E}_y, \mathscr{E}_z\}$ is the electric field vector, $\boldsymbol{C}^{\mathscr{E}}$ is the stiffness matrix calculated at constant $\mathscr{E}$, $\boldsymbol{e}$ is the piezoelectric matrix that couples electrical and mechanical fields, and $\boldsymbol{\varepsilon}^{\epsilon} = \{\varepsilon_{xx}, \varepsilon_{yy}, \varepsilon_{zz}\}$ is the permittivity matrix calculated at ϵ-constant.

The constitutive equations will be written out in Section 3 in a form suitable for the F-RMVT application.

Geometrical relations. The strain-displacement geometrical (subscript G) relations in the linear case are

$$\boldsymbol{\epsilon}^k_{pG} = \boldsymbol{D}_p\, \boldsymbol{u}^k, \quad \boldsymbol{\epsilon}^k_{nG} = (\boldsymbol{D}_{np} + \boldsymbol{D}_{nz})\boldsymbol{u}^k. \tag{2}$$

The superscript k is the layer index. Strains have been split into in-plane (subscript p) and out-of-plane (subscript n, for "normal") components:

$$\boldsymbol{\epsilon}^k_p = \{\epsilon_{xx}, \epsilon_{yy}, \epsilon_{xy}\}, \quad \boldsymbol{\epsilon}^k_n = \{\epsilon_{xz}, \epsilon_{yz}, \epsilon_{zz}\},$$

while $\boldsymbol{u}^k = \{u_x, u_y, u_z\}$ is the vector of the displacement components. The differential matrices are given explicitly by

$$\boldsymbol{D}_p = \begin{bmatrix} \partial_x & 0 & 0 \\ 0 & \partial_y & 0 \\ \partial_y & \partial_x & 0 \end{bmatrix}, \quad \boldsymbol{D}_{np} = \begin{bmatrix} 0 & 0 & \partial_x \\ 0 & 0 & \partial_y \\ 0 & 0 & 0 \end{bmatrix}, \quad \boldsymbol{D}_{nz} = \begin{bmatrix} \partial_z & 0 & 0 \\ 0 & \partial_z & 0 \\ 0 & 0 & \partial_z \end{bmatrix}. \tag{3}$$

The electric field $\mathscr{E}$ is related to the electric potential by the gradient relation

$$\mathscr{E}^{kT} = \begin{bmatrix} -\partial_x & -\partial_y & -\partial_z \end{bmatrix} \Phi^k. \tag{4}$$

The electric potential Φ being a scalar, one obtains by separating in-plane and normal components the equality

$$\mathscr{E}^k = \Big(\boldsymbol{D}_{ep} + \boldsymbol{D}_{ez}\Big)\Phi^k, \tag{5}$$

where

$$\boldsymbol{D}^T_{ep} = \begin{bmatrix} -\partial_x & -\partial_y & 0 \end{bmatrix}, \quad \boldsymbol{D}^T_{ez} = \begin{bmatrix} 0 & 0 & -\partial_z \end{bmatrix}. \tag{6}$$

3. Variational statements for piezoelectric continua

The classical variational tool most often used to develop FEs, is the principle of virtual displacements (PVD), which, for a piezoelectric continuum, can be written

$$\sum_{k=1}^{N_l} \int_{\Omega_k} \int_{A_k} \left(\delta\boldsymbol{\epsilon}^{kT}_{pG}\boldsymbol{\sigma}^k_{pC} + \delta\boldsymbol{\epsilon}^{kT}_{nG}\boldsymbol{\sigma}^k_{nC} - \delta\mathscr{E}^{kT}_G \mathscr{D}^k_C\right) d\Omega_k\, dz = \delta L_e. \tag{7}$$

Here δ denotes virtual variations, A_k is the layer domain in the thickness direction, Ω_k denotes the reference surface of the layer, and δL_e denotes the virtual variation of the work made by applied loadings. The in-plane and out-of-plane stress components are

$$\boldsymbol{\sigma}^T_p = \{\sigma_{xx}, \sigma_{yy}, \sigma_{xy}\}, \quad \boldsymbol{\sigma}^T_n = \{\sigma_{xz}, \sigma_{yz}, \sigma_{zz}\}.$$

The electrical work is obtained via the electrical displacement vector:

$$\mathscr{D} = \{\mathscr{D}_x, \mathscr{D}_y, \mathscr{D}_z\}.$$

A subscript C will denote stress and electrical displacements from the constitutive law, and a subscript G strains and electrical fields from the geometrical relation. The PVD allows one to assume two independent fields for $\boldsymbol{u}$ and Φ. The remaining variables are obtained from the constitutive law of the piezoelectric layers.

The RMVT was proposed in [Reissner 1984] for purely mechanical problems. A critical review on its use was given in [Carrera 2001]. A main feature of the RMVT is that it allows one to assume two independent fields for displacements $\boldsymbol{u}$ and transverse stresses $\boldsymbol{\sigma}_n$. This allows the *a priori* fulfillment of the necessary continuity (equilibrium) conditions of transverse normal and shear stresses at each layer interfaces. In the static case, for pure mechanical problems RMVT states that

$$\sum_{k=1}^{N_l} \int_{\Omega_k} \int_{A_k} \left(\delta \boldsymbol{\epsilon}_{pG}^{kT} \boldsymbol{\sigma}_{pC}^{k} + \delta \boldsymbol{\epsilon}_{nG}^{kT} \boldsymbol{\sigma}_{nM}^{k} - \delta \boldsymbol{\sigma}_{nM}^{kT} (\boldsymbol{\epsilon}_{nG}^{k} - \boldsymbol{\epsilon}_{nC}^{k}) \right) d\Omega_k \, dz = \delta L_e. \tag{8}$$

The second term in the integrand forces the compatibility of transverse strain obtained by the material's constitutive law (which are different from those related to PVD applications) and by the geometric relation. The subscript M denotes those variables which are assumed in a given model.

By introducing the electrical work, we can write the RMVT for piezoelectric continua as

$$\sum_{k=1}^{N_l} \int_{\Omega_k} \int_{A_k} \left(\delta \boldsymbol{\epsilon}_{pG}^{kT} \boldsymbol{\sigma}_{pC}^{k} + \delta \boldsymbol{\epsilon}_{nG}^{kT} \boldsymbol{\sigma}_{nM}^{k} - \delta \mathscr{E}_{G}^{kT} \mathscr{D}_{C}^{k} - \delta \boldsymbol{\sigma}_{nM}^{kT} (\boldsymbol{\epsilon}_{nG}^{k} - \boldsymbol{\epsilon}_{nC}^{k}) \right) d\Omega_k \, dz = \delta L_e. \tag{9}$$

This form of the RMVT will be called the *partial* extension of RMVT to piezoelectric continua, or P-RMVT.

A full extension of the RMVT can be obtained by introducing the transverse components of electric displacement $\mathscr{D}_z$ as additional variables. The RMVT then assumes the following *full* form, or F-RMVT:

$$\sum_{k=1}^{N_l} \int_{Ak} \int_{hk} \left(\delta \boldsymbol{\epsilon}_{pG}^{kT} \boldsymbol{\sigma}_{pC}^{k} + \delta \boldsymbol{\epsilon}_{nG}^{kT} \boldsymbol{\sigma}_{nM}^{k} - \delta \mathscr{E}_{pG}^{kT} \mathscr{D}_{pC}^{k} - \delta \mathscr{E}_{nG}^{kT} \mathscr{D}_{nM}^{k} + \delta \boldsymbol{\sigma}_{nM}^{kT} (\boldsymbol{\epsilon}_{nG}^{k} - \boldsymbol{\epsilon}_{nC}^{k}) \right.$$
$$\left. - \mathscr{D}_{nM}^{T} (\mathscr{E}_{nG}^{k} - \mathscr{E}_{nC}^{k}) \right) dA_k \, dz = \delta L_e. \tag{10}$$

The electrical displacement and electrical field vectors have been split into in-plane and normal components (as for the stresses $\boldsymbol{\sigma}$ and strains $\boldsymbol{\epsilon}$):

$$\mathscr{D}_p = \{\mathscr{D}_x, \mathscr{D}_y\}, \quad \mathscr{D}_n = \{\mathscr{D}_z\}, \quad \mathscr{E}_p = \{E_x, \mathscr{E}_y\}, \quad \mathscr{E}_n = \{\mathscr{E}_z\}.$$

The constitutive equations of the k-layer are conveniently written as

$$\begin{aligned} \boldsymbol{\sigma}_{pC}^{k} &= \boldsymbol{C}_{pp}^{k} \boldsymbol{\epsilon}_{pG}^{k} + \boldsymbol{C}_{pn}^{k} \boldsymbol{\epsilon}_{nC}^{k} - \boldsymbol{e}_{pp}^{k\,T} \mathscr{E}_{pG}^{k} - \boldsymbol{e}_{np}^{k\,T} \mathscr{E}_{nC}^{k}, \quad & \mathscr{D}_{pC}^{k} &= \boldsymbol{e}_{pp}^{k} \boldsymbol{\epsilon}_{pG}^{k} + \boldsymbol{e}_{pn}^{k} \boldsymbol{\epsilon}_{nC}^{k} + \boldsymbol{\varepsilon}_{pp}^{k} \mathscr{E}_{pG}^{k} + \boldsymbol{\varepsilon}_{pn}^{k} \mathscr{E}_{nC}^{k}, \\ \boldsymbol{\sigma}_{nM}^{k} &= \boldsymbol{C}_{pn}^{k\,T} \boldsymbol{\epsilon}_{pG}^{k} + \boldsymbol{C}_{nn}^{k} \boldsymbol{\epsilon}_{nC}^{k} - \boldsymbol{e}_{pn}^{k\,T} \mathscr{E}_{pG}^{k} - \boldsymbol{e}_{nn}^{k\,T} \mathscr{E}_{nC}^{k}, \quad & \mathscr{D}_{nC}^{k} &= \boldsymbol{e}_{np}^{k} \boldsymbol{\epsilon}_{pG}^{k} + \boldsymbol{e}_{nn}^{k} \boldsymbol{\epsilon}_{nC}^{k} + \boldsymbol{\varepsilon}_{pn}^{k\,T} \mathscr{E}_{pG}^{k} + \boldsymbol{\varepsilon}_{nn}^{k} \mathscr{E}_{nC}^{k}, \end{aligned} \tag{11}$$

where we have introduced the following arrays:

- Stiffness matrices:

$$\boldsymbol{C}^k_{pp} = \begin{bmatrix} C_{11} & C_{12} & C_{16} \\ C_{12} & C_{22} & C_{26} \\ C_{16} & C_{26} & C_{66} \end{bmatrix}^k, \quad \boldsymbol{C}^k_{pn} = \begin{bmatrix} 0 & 0 & C_{13} \\ 0 & 0 & C_{23} \\ 0 & 0 & C_{36} \end{bmatrix}^k, \quad \boldsymbol{C}^k_{nn} = \begin{bmatrix} C_{55} & C_{45} & 0 \\ C_{45} & C_{44} & 0 \\ 0 & 0 & C_{33} \end{bmatrix}^k. \tag{12}$$

- Piezoelectric matrices:

$$\boldsymbol{e}^k_{pp} = \begin{bmatrix} 0 & 0 & 0 \\ 0 & 0 & 0 \end{bmatrix}^k, \quad \boldsymbol{e}^k_{pn} = \begin{bmatrix} e_{15} & e_{14} & 0 \\ e_{25} & e_{24} & 0 \end{bmatrix}^k, \quad \boldsymbol{e}^k_{np} = \begin{bmatrix} e_{31} & e_{32} & e_{33} \end{bmatrix}^k, \quad \boldsymbol{e}^k_{nn} = \begin{bmatrix} 0 & 0 & e_{33} \end{bmatrix}^k. \tag{13}$$

- Permittivity matrices:

$$\boldsymbol{\varepsilon}^k_{pp} = \begin{bmatrix} \varepsilon_{11} & \varepsilon_{12} \\ \varepsilon_{12} & \varepsilon_{22} \end{bmatrix}^k, \quad \boldsymbol{\varepsilon}^k_{pn} = \begin{bmatrix} 0 \\ 0 \end{bmatrix}^k, \quad \boldsymbol{\varepsilon}^k_{nn} = \begin{bmatrix} \varepsilon_{33} \end{bmatrix}^k. \tag{14}$$

Application of the F-RMVT requires one to express the in-plane stresses $\boldsymbol{\sigma}_{pC}$, the normal strains $\boldsymbol{\epsilon}_{nC}$, the normal electric field $\mathscr{E}_{nC}$ and the in-plane electric displacements $\mathscr{D}_{pC}$ in terms of the remaining variables. Thus the constitutive equations (11) can be solved as follows:

$$\begin{aligned} \boldsymbol{\sigma}_{pC} &= \hat{\boldsymbol{C}}_{spm}\boldsymbol{\epsilon}_{pG} + \hat{\boldsymbol{C}}_{snm}\boldsymbol{\sigma}_{nM} + \hat{\boldsymbol{C}}_{spe}\mathscr{E}_{pG} + \hat{\boldsymbol{C}}_{sne}\mathscr{D}_{nM}, \\ \boldsymbol{\epsilon}_{nC} &= \hat{\boldsymbol{C}}_{dpm}\boldsymbol{\epsilon}_{pG} + \hat{\boldsymbol{C}}_{dnm}\boldsymbol{\sigma}_{nM} + \hat{\boldsymbol{C}}_{dpe}\mathscr{E}_{pG} + \hat{\boldsymbol{C}}_{dne}\mathscr{D}_{nM}, \\ \mathscr{D}_{pC} &= \hat{\boldsymbol{C}}_{fpm}\boldsymbol{\epsilon}_{pG} + \hat{\boldsymbol{C}}_{fnm}\boldsymbol{\sigma}_{nM} + \hat{\boldsymbol{C}}_{fpe}\mathscr{E}_{pG} + \hat{\boldsymbol{C}}_{fne}\mathscr{D}_{nM}, \\ \boldsymbol{E}_{nC} &= \hat{\boldsymbol{C}}_{epm}\boldsymbol{\epsilon}_{pG} + \hat{\boldsymbol{C}}_{enm}\boldsymbol{\sigma}_{nM} + \hat{\boldsymbol{C}}_{epe}\mathscr{E}_{pG} + \hat{\boldsymbol{C}}_{ene}\mathscr{D}_{nM}. \end{aligned} \tag{15}$$

The matrices above are obtained from by those in (11) by means of the relations

$$\begin{aligned} \bar{\boldsymbol{C}}^k_{dpm} &= -\boldsymbol{C}^{k\,-1}_{nn}\boldsymbol{C}^{kT}_{pn} - \left(\boldsymbol{C}^{k\,-1}_{nn}\boldsymbol{e}^{kT}_{nn}\right)\left(\boldsymbol{e}^k_{nn}\boldsymbol{C}^{k\,-1}_{nn}\boldsymbol{e}^{kT}_{nn} + \boldsymbol{\varepsilon}^k_{nn}\right)^{-1}\left(\boldsymbol{e}^k_{np} - \boldsymbol{e}^k_{nn}\boldsymbol{C}^{k\,-1}_{nn}\boldsymbol{C}^{kT}_{pn}\right), \\ \bar{\boldsymbol{C}}^k_{dnm} &= \boldsymbol{C}^{k\,-1}_{nn} - \left(\boldsymbol{C}^{k\,-1}_{nn}\boldsymbol{e}^{kT}_{nn}\right)\left(\boldsymbol{e}^k_{nn}\boldsymbol{C}^{k\,-1}_{nn}\boldsymbol{e}^{kT}_{nn} + \boldsymbol{\varepsilon}^k_{nn}\right)^{-1}\left(\boldsymbol{e}^k_{nn}\boldsymbol{C}^{k\,-1}_{nn}\right), \\ \bar{\boldsymbol{C}}^k_{dpe} &= \boldsymbol{C}^{k\,-1}_{nn}\boldsymbol{e}^{kT}_{pn} - \left(\boldsymbol{C}^{k\,-1}_{nn}\boldsymbol{e}^{kT}_{nn}\right)\left(\boldsymbol{e}^k_{nn}\boldsymbol{C}^{k\,-1}_{nn}\boldsymbol{e}^{kT}_{nn} + \boldsymbol{\varepsilon}^k_{nn}\right)^{-1}\left(\boldsymbol{e}^k_{nn}\boldsymbol{C}^{k\,-1}_{nn}\boldsymbol{e}^{kT}_{pn} + \boldsymbol{\varepsilon}^{kT}_{pn}\right), \\ \bar{\boldsymbol{C}}^k_{dne} &= \left(\boldsymbol{C}^{k\,-1}_{nn}\boldsymbol{e}^{kT}_{nn}\right)\left(\boldsymbol{e}^k_{nn}\boldsymbol{C}^{k\,-1}_{nn}\boldsymbol{e}^{kT}_{nn} + \boldsymbol{\varepsilon}^k_{nn}\right)^{-1}, \\ \bar{\boldsymbol{C}}^k_{epm} &= -\left(\boldsymbol{e}^k_{nn}\boldsymbol{C}^{k\,-1}_{nn}\boldsymbol{e}^{kT}_{nn} + \boldsymbol{\varepsilon}^k_{nn}\right)^{-1}\left(\boldsymbol{e}^k_{np} - \boldsymbol{e}^k_{nn}\boldsymbol{C}^{k\,-1}_{nn}\boldsymbol{C}^{kT}_{pn}\right), \\ \bar{\boldsymbol{C}}^k_{enm} &= -\left(\boldsymbol{e}^k_{nn}\boldsymbol{C}^{k\,-1}_{nn}\boldsymbol{e}^{kT}_{nn} + \boldsymbol{\varepsilon}^k_{nn}\right)^{-1}\left(\boldsymbol{e}^k_{nn}\boldsymbol{C}^{k\,-1}_{nn}\right), \\ \bar{\boldsymbol{C}}^k_{epe} &= -\left(\boldsymbol{e}^k_{nn}\boldsymbol{C}^{k\,-1}_{nn}\boldsymbol{e}^{kT}_{nn} + \boldsymbol{\varepsilon}^k_{nn}\right)^{-1}\left(\boldsymbol{e}^k_{nn}\boldsymbol{C}^{k\,-1}_{nn}\boldsymbol{e}^{kT}_{pn} + \boldsymbol{\varepsilon}^{kT}_{pn}\right), \\ \bar{\boldsymbol{C}}^k_{ene} &= \left(\boldsymbol{e}^k_{nn}\boldsymbol{C}^{k\,-1}_{nn}\boldsymbol{e}^{kT}_{nn} + \boldsymbol{\varepsilon}^k_{nn}\right)^{-1}, \\ \bar{\boldsymbol{C}}^k_{spm} &= \boldsymbol{C}^k_{pp} + \boldsymbol{C}^k_{pn}\bar{\boldsymbol{C}}^k_{dpm} - \boldsymbol{e}^{kT}_{np}\bar{\boldsymbol{C}}^k_{epm}, & \bar{\boldsymbol{C}}^k_{snm} &= \boldsymbol{C}^k_{pn}\bar{\boldsymbol{C}}^k_{dnm} - \boldsymbol{e}^{kT}_{np}\bar{\boldsymbol{C}}^k_{enm}, \\ \bar{\boldsymbol{C}}^k_{spe} &= \boldsymbol{C}^k_{pn}\bar{\boldsymbol{C}}^k_{dpe} - \boldsymbol{e}^{kT}_{pp} - \boldsymbol{e}^{kT}_{np}\bar{\boldsymbol{C}}^k_{epe}, & \bar{\boldsymbol{C}}^k_{sne} &= \boldsymbol{C}^k_{pn}\bar{\boldsymbol{C}}^k_{dne} - \boldsymbol{e}^{kT}_{np}\bar{\boldsymbol{C}}^k_{ene}, \\ \bar{\boldsymbol{C}}^k_{fpm} &= \boldsymbol{e}^k_{pp} + \boldsymbol{e}^k_{pn}\bar{\boldsymbol{C}}^k_{dpm} + \boldsymbol{\varepsilon}^k_{np}\bar{\boldsymbol{C}}^k_{epm}, & \bar{\boldsymbol{C}}^k_{fnm} &= \boldsymbol{e}^k_{pn}\bar{\boldsymbol{C}}^k_{dnm} + \boldsymbol{\varepsilon}^k_{pn}\bar{\boldsymbol{C}}^k_{enm}, \\ \bar{\boldsymbol{C}}^k_{fpe} &= \boldsymbol{e}^k_{pn}\bar{\boldsymbol{C}}^k_{dpe} + \boldsymbol{\varepsilon}^k_{pp} + \boldsymbol{\varepsilon}^k_{pn}\bar{\boldsymbol{C}}^k_{epe}, & \bar{\boldsymbol{C}}^k_{fne} &= \boldsymbol{e}^k_{pn}\bar{\boldsymbol{C}}^k_{dne} + \boldsymbol{\varepsilon}^k_{pn}\bar{\boldsymbol{C}}^k_{ene}. \end{aligned}$$

It must be noted that

$$\hat{\boldsymbol{C}}^k_{dnm} = \hat{\boldsymbol{C}}^{kT}_{dnm}, \qquad \hat{\boldsymbol{C}}^k_{spm} = \hat{\boldsymbol{C}}^{kT}_{spm}, \qquad \hat{\boldsymbol{C}}^k_{fpe} = \hat{\boldsymbol{C}}^{kT}_{fpe}, \qquad \hat{\boldsymbol{C}}^k_{ene} = \hat{\boldsymbol{C}}^{kT}_{ene},$$
$$\hat{\boldsymbol{C}}^k_{dpm} = -\hat{\boldsymbol{C}}^{kT}_{snm}, \qquad \hat{\boldsymbol{C}}^k_{dne} = \hat{\boldsymbol{C}}^{kT}_{enm}, \qquad \hat{\boldsymbol{C}}^k_{dpe} = \hat{\boldsymbol{C}}^{kT}_{fnm}, \qquad \hat{\boldsymbol{C}}^k_{epm} = \hat{\boldsymbol{C}}^{kT}_{sne}.$$

4. Unified formulation for plate elements

The unified formulation is a technique that allows one to handle in a unified manner a large variety of plate modelings and finite elements. In this formulation, the finite element matrices are written in terms of a few *fundamental nuclei*, which do not formally depend on: the expansion N used in the z-direction, the number of the node N_n of the element, or the variables description (LW or ESL).

The unknown variables $\boldsymbol{u}$, $\boldsymbol{\sigma}_n$, Φ and $\mathcal{D}_z$ are expressed in terms of the layer thickness coordinate:

$$\begin{aligned}\left(\boldsymbol{u}^k(x,y,z),\varphi^k(x,y,z),\boldsymbol{\sigma}^k_n(x,y,z),\mathcal{D}^k_n(x,y,z)\right) &= F_b(z)\left(\boldsymbol{u}^k_b(x,y),\varphi^k_b(x,y),\boldsymbol{\sigma}^k_{nb}(x,y),\mathcal{D}^k_{nb}(x,y)\right)\\ &+ F_r(z)\left(\boldsymbol{u}^k_r(x,y),\varphi^k_r(x,y),\boldsymbol{\sigma}^k_{nr}(x,y),\mathcal{D}^k_{nr}(x,y)\right) + F_t(z)\left(\boldsymbol{u}^k_t(x,y),\varphi^k_t(x,y),\boldsymbol{\sigma}^k_{nt}(x,y),\mathcal{D}^k_{nt}(x,y)\right). \quad (16)\end{aligned}$$

The subscript t and b denote the linear part of the thickness expansion (t and b will be used to denote top- and bottom-layer variable values in layerwise cases), while subscript r refers to higher-order terms: $r = 2, \ldots, N-1$. In compact form,

$$\left(\boldsymbol{u}^k(x,y,z),\varphi^k(x,y,z),\boldsymbol{\sigma}^k_n(x,y,z),\mathcal{D}^k_n(x,y,z)\right) = F_\tau(z)\left(\boldsymbol{u}^k(x,y),\varphi^k(x,y),\boldsymbol{\sigma}^k_n(x,y),\mathcal{D}^k_n(x,y)\right)_\tau. \quad (17)$$

Here $\left(\boldsymbol{u}^k(x,y),\phi^k(x,y),\boldsymbol{\sigma}^k_n(x,y),\mathcal{D}^k_n(x,y)\right)_\tau$ are two-dimensional unknowns, the $F_\tau(z)$ are the base functions of the expansion, and the summation convention over repeated index has been adopted. The base functions could be, in general, different for each variable. Different choices for $F_\tau(z)$ will lead to different plate/shell theories. The choices made in our study are briefly discussed below; detailed descriptions can be found in the works cited.

. Layer-wise elements.

The thickness functions are given by combinations of Legendre polynomials P_j as

$$F_t = \frac{P_0(\zeta_k) + P_1(\zeta_k)}{2}, \quad F_b = \frac{P_0(\zeta_k) - P_1(\zeta_k)}{2}, \quad F_r = P_r(\zeta_k) - P_{r-2}(\zeta_k), \quad r = 2, 3, \ldots, N, \quad (18)$$

for $\zeta = z_k/2h_k$, where z_k is the local layer thickness coordinate and h_k is the layer thickness, so $-1 \le \zeta_k \le 1$. As mentioned, t and b denote top and bottom; that is, the chosen functions have the properties

$$\zeta_k = \begin{cases} 1 \ : \ F_t = 1, \ F_b = 0, \ F_r = 0, \\ -1 \ : \ F_t = 0, \ F_b = 1, \ F_r = 0, \end{cases} \quad (19)$$

Thanks to these properties the interlaminar continuity of the assumed variables can be easily linked in the assembly procedure from layer-level matrices to multilayer-level matrices.

The resulting elements will be denoted by the acronyms LFM1 to LFM4, in which L means layerwise, FM states that F-RMVT has been employed, and the digit is the order of the expansion. Particular cases of P-RMVT and PVD will also be used in the numerical analysis; these applications will be denoted by LPM1 to LPM4 and LD1 to LD4, respectively.

Equivalent single-layer model. In this case the layerwise expansion is preserved for the transverse stresses, electric potential and electric displacements, while a Taylor-type expansion is used for the displacement components:

$$\boldsymbol{u}(x, y, z) = \boldsymbol{u}_\tau(x, y)\, z^\tau, \quad \tau = 0, N$$

The base functions related to displacements can be chosen as

$$F_b(z) = 1, \quad F_r(z) = z^r, \quad r = 1, N-1, \quad F_t(z) = z^N.$$

These theories will be denoted with the acronyms EFMC1 to EFMC3, in which E means equivalent single-layer, FM means full mixed, and C that interlaminar continuity conditions are fulfilled for transverse stresses, electric potential and transverse electric displacement. The digit, as before, denotes the expansion order. Results related to P-RMVT application will be denoted by EPMC1 to EPMC3. When the Murakami zigzag function is used (which allows the introduction of piecewise continuous displacement fields in the thickness plate direction; see [Carrera 2001]), the resulting elements are referred to as EFMZC1 to EFMZC3 and EPMZC1 to EPMZC3 for the full and partial cases.

Finite element approximations. Finite element approximations to the plate reference surface domain are introduced by means of isoparametric descriptions for the various field variables:

$$\left(\boldsymbol{u}_\tau^k, \boldsymbol{\Phi}_\tau^k, \boldsymbol{\sigma}_{n\tau}^k, \mathcal{D}_{n\tau}^k\right)(x, y) = N_i(x, y)\left(\boldsymbol{q}_{\tau i}^k, g_{\tau i}^k, \boldsymbol{f}_{\tau i}^k, d_{\tau i}^k\right), \quad i = 1, 2, \ldots, N_n, \tag{20}$$

where the $N_i(x, y)$ are the shape functions, $\boldsymbol{q}_{\tau i}^k$ the nodal unknown displacements, $g_{\tau i}^k$ the nodal unknown electric potentials, $\boldsymbol{f}_{\tau i}^k$ the nodal unknowns normal stresses and $d_{\tau i}^k$ the nodal unknown normal electrical displacements. The cases of 9, 8 and 4 nodes are considered in the numerical implementation referred to as Q9, Q8 and Q4 finite elements [Carrera and DeMasi 2002b].

5. Derivation of finite element matrices

This section is devoted to the fundamental nuclei of the F-RMVT finite element matrices. The RMVT and PVD matrices can be found in [Carrera and DeMasi 2002a; Carrera and Boscolo 2006].

By starting from Equation (10), the fundamental nuclei are derived in several steps:

1. The constitutive relations (15) are introduced in the F-RMVT statement at (10).
2. The geometric relations are used to express strain in terms of displacements and electric field in terms of electric potential.
3. The through-the-thickness assumptions by means of the Unified Formulation are introduced.
4. The FE shape functions are used to eliminate the in-plane plate coordinates by numerical integration.
5. Matrix products are made, yielding the explicit forms of the fundamental nuclei.

We omit the details for brevity. The final form of the governing equations is

$$\begin{aligned}
\delta \boldsymbol{q}_{\tau i}^{k\,T}: &\quad \boldsymbol{K}_{uu}^{k\tau sij}\boldsymbol{q}_{sj}^{k}+\boldsymbol{K}_{u\sigma}^{k\tau sij}\boldsymbol{f}_{sj}^{k}+\boldsymbol{K}_{ue}^{k\tau sij}g_{sj}^{k}+\boldsymbol{K}_{ud}^{k\tau sij}d_{sj}^{k}=\boldsymbol{P}_{u\tau}^{k},\\
\delta \boldsymbol{f}_{\tau i}^{kT}: &\quad \boldsymbol{K}_{\sigma u}^{k\tau sij}\boldsymbol{q}_{sj}^{k}+\boldsymbol{K}_{\sigma\sigma}^{k\tau sij}\boldsymbol{f}_{sj}^{k}+\boldsymbol{K}_{\sigma e}^{k\tau sij}g_{sj}^{k}+\boldsymbol{K}_{\sigma d}^{k\tau sij}d_{sj}^{k}=0,\\
\delta g_{\tau i}^{k\,T}: &\quad \boldsymbol{K}_{eu}^{k\tau sij}\boldsymbol{q}_{sj}^{k}+\boldsymbol{K}_{e\sigma}^{k\tau sij}\boldsymbol{f}_{sj}^{k}+\boldsymbol{K}_{ee}^{k\tau sij}g_{sj}^{k}+\boldsymbol{K}_{ed}^{k\tau sij}d_{sj}^{k}=\boldsymbol{P}_{e\tau}^{k},\\
\delta d_{\tau i}^{k\,T}: &\quad \boldsymbol{K}_{du}^{k\tau sij}\boldsymbol{q}_{sj}^{k}+\boldsymbol{K}_{d\sigma}^{k\tau sij}\boldsymbol{f}_{sj}^{k}+\boldsymbol{K}_{de}^{k\tau sij}g_{sj}^{k}+\boldsymbol{K}_{dd}^{k\tau sij}d_{sj}^{k}=0.
\end{aligned}\tag{21}$$

The mechanical and electrical loading terms on the right-hand side are

$$\boldsymbol{P}_{u\tau}^{k}=\boldsymbol{K}_{up}^{k\tau sij}\boldsymbol{p}_{sj},\quad \boldsymbol{P}_{e\tau}^{k}=-\boldsymbol{K}_{ef}^{k\tau sij}\Psi_{sj}.\tag{22}$$

The explicit forms of the fundamental nuclei thus obtained are

$$\begin{aligned}
\boldsymbol{K}_{uu}^{k\tau sij}&=\int_{\Omega}\left(\boldsymbol{D}_{p}^{T}N_i\hat{\boldsymbol{C}}_{spm}^{k}E_{\tau s}^{uu}\boldsymbol{D}_{p}N_j\right)d\Omega,\\
\boldsymbol{K}_{u\sigma}^{k\tau sij}&=\int_{\Omega}\left(\boldsymbol{D}_{p}^{T}N_i\hat{\boldsymbol{C}}_{snm}^{k}E_{\tau s}^{u\sigma}N_j+N_i\boldsymbol{D}_{np}^{T}E_{\tau s}^{u\sigma}N_j+N_i\boldsymbol{I}^{T}E_{\tau,zs}^{u\sigma}N_j\right)d\Omega,\\
\boldsymbol{K}_{ue}^{k\tau sij}&=\int_{\Omega}\left(\boldsymbol{D}_{p}^{T}N_i\hat{\boldsymbol{C}}_{spe}^{k}E_{\tau s}^{ue}\boldsymbol{D}_{ep}N_j\right)d\Omega,\\
\boldsymbol{K}_{ud}^{k\tau sij}&=\int_{\Omega}\left(\boldsymbol{D}_{p}^{T}N_i\hat{\boldsymbol{C}}_{sne}^{k}E_{\tau s}^{ue}N_j\right)d\Omega,\\
\boldsymbol{K}_{\sigma u}^{k\tau sij}&=\int_{\Omega}\left(N_iE_{\tau s}^{\sigma u}\boldsymbol{D}_{np}N_j+N_iE_{\tau s,z}^{\sigma u}\boldsymbol{I}N_j-N_i\hat{\boldsymbol{C}}_{dpm}^{k}E_{\tau s}^{\sigma u}\boldsymbol{D}_{p}N_j\right)d\Omega,\\
\boldsymbol{K}_{\sigma\sigma}^{k\tau sij}&=-\int_{\Omega}\left(N_i\hat{\boldsymbol{C}}_{dnm}^{k}E_{\tau s}^{\sigma\sigma}N_j\right)d\Omega,\\
\boldsymbol{K}_{\sigma e}^{k\tau sij}&=-\int_{\Omega}\left(N_i\hat{\boldsymbol{C}}_{dpe}^{k}E_{\tau s}^{\sigma e}\boldsymbol{D}_{ep}N_j\right)d\Omega,\\
\boldsymbol{K}_{\sigma d}^{k\tau sij}&=-\int_{\Omega}\left(N_i\hat{\boldsymbol{C}}_{dne}^{k}E_{\tau s}^{\sigma e}N_j\right)d\Omega,\\
\boldsymbol{K}_{eu}^{k\tau sij}&=-\int_{\Omega}\left(\boldsymbol{D}_{ep}^{T}N_i\hat{\boldsymbol{C}}_{fpm}^{k}E_{\tau s}^{eu}\boldsymbol{D}_{p}N_j\right)d\Omega,\\
\boldsymbol{K}_{e\sigma}^{k\tau sij}&=-\int_{\Omega}\left(N_i\boldsymbol{D}_{ep}^{T}\hat{\boldsymbol{C}}_{fnm}^{k}E_{\tau s}^{e\sigma}N_j\right)d\Omega,\\
\boldsymbol{K}_{ee}^{k\tau sij}&=-\int_{\Omega}\left(N_i\boldsymbol{D}_{ep}^{T}\hat{\boldsymbol{C}}_{fpe}^{k}E_{\tau s}^{ee}\boldsymbol{D}_{ep}N_j\right)d\Omega,\\
\boldsymbol{K}_{ed}^{k\tau sij}&=-\int_{\Omega}\left(N_i\boldsymbol{D}_{ep}^{T}\hat{\boldsymbol{C}}_{fne}^{k}E_{\tau s}^{ee}\boldsymbol{D}_{ep}N_j+\boldsymbol{I}^{*}N_iE_{\tau,zs}^{\sigma e}N_j\right)d\Omega,\\
\boldsymbol{K}_{du}^{k\tau sij}&=\int_{\Omega}\left(N_i\hat{\boldsymbol{C}}_{epm}^{k}E_{\tau s}^{du}\boldsymbol{D}_{p}N_j\right)d\Omega,\\
\boldsymbol{K}_{d\sigma}^{k\tau sij}&=\int_{\Omega}\left(N_i\hat{\boldsymbol{C}}_{enm}^{k}E_{\tau s}^{d\sigma}N_j\right)d\Omega,
\end{aligned}$$

$$\boldsymbol{K}_{de}^{k\tau sij} = \int_\Omega \left(- N_i E_{\tau s,z}^{d\phi} \boldsymbol{I}^* N_j + N_i \hat{\boldsymbol{C}}_{epe}^{k} E_{\tau s}^{d\phi} \boldsymbol{D}_{ep} N_j \right) d\Omega,$$

$$\boldsymbol{K}_{dd}^{k\tau sij} = \int_\Omega \left(N_i \hat{\boldsymbol{C}}_{ene}^{k} E_{\tau s}^{dd} N_j \right) d\Omega,$$

$$\boldsymbol{K}_{up}^{k\tau sij} = \int_\Omega F_\tau^1 \left(N_i N_j \boldsymbol{m}_s^k \right) F_s^1 \, d\Omega,$$

$$\boldsymbol{K}_{ef}^{k\tau sij} = \int_\Omega F_\tau^1 \left(N_i N_j n_s^k \right) F_s^1 \, d\Omega.$$

$\boldsymbol{I}$ is the unit matrix and $\boldsymbol{I}^{\star T} = \{0, 0, -1\}$. The following integrals have been defined:

$$E_{\tau s}^{\alpha\beta} = \int_{A_k} F_\tau^\alpha F_s^\beta \, dz, \quad E_{\tau,zs}^{\alpha\beta} = \int_{A_k} F_{\tau,z}^\alpha F_s^\beta \, dz, \quad E_{\tau s,z}^{\alpha\beta} = \int_{A_k} F_\tau^\alpha F_{s,z}^\beta \, dz,$$

where α and β can assume any of the values $u, \sigma, \Phi, \mathcal{D}$ to denote thickness function used for the related variables.

Table 1 summarizes the dimensions of the nuclei. By varying the subscripts τ, s, k, i, j over their ranges one obtains the element matrices; see [Carrera 2003b].

$\boldsymbol{K}_{uu}^{k\tau sij}$	$[3\times3]$	$\boldsymbol{K}_{eu}^{k\tau sij}$	$[1\times3]$	$\boldsymbol{K}_{\sigma u}^{k\tau sij}$	$[3\times3]$	$\boldsymbol{K}_{du}^{k\tau sij}$	$[1\times3]$
$\boldsymbol{K}_{u\sigma}^{k\tau sij}$	$[3\times3]$	$\boldsymbol{K}_{e\sigma}^{k\tau sij}$	$[1\times3]$	$\boldsymbol{K}_{\sigma\sigma}^{k\tau sij}$	$[3\times3]$	$\boldsymbol{K}_{d\sigma}^{k\tau sij}$	$[1\times3]$
$\boldsymbol{K}_{ue}^{k\tau sij}$	$[3\times1]$	$\boldsymbol{K}_{ee}^{k\tau sij}$	$[1\times1]$	$\boldsymbol{K}_{\sigma e}^{k\tau sij}$	$[3\times1]$	$\boldsymbol{K}_{de}^{k\tau sij}$	$[1\times1]$
$\boldsymbol{K}_{ud}^{k\tau sij}$	$[3\times1]$	$\boldsymbol{K}_{ed}^{k\tau sij}$	$[1\times1]$	$\boldsymbol{K}_{\sigma d}^{k\tau sij}$	$[3\times1]$	$\boldsymbol{K}_{dd}^{k\tau sij}$	$[1\times1]$
$\boldsymbol{K}_{ef}^{k\tau sij}$	$[1\times1]$	$\boldsymbol{K}_{up}^{k\tau sij}$	$[3\times3]$			$\boldsymbol{M}_{u\ddot{u}}^{k\tau sij}$	$[3\times3]$

Table 1. Dimensions of the fundamental nuclei.

6. Numerical results

This section shows the performance of the mixed FEs developed on the basis of interlaminar *a priori* continuous transversal electric displacements $\mathcal{D}_z$, comparing it with a mixed elements approach that does not incorporate such continuity, as with one based of PVD applications. Further comparisons are given with the results in [Garcia Lage et al. 2004b] and with three dimensional solutions in [Heyliger 1994]. To compare the analysis with closed-form exact solutions, attention has been restricted to simply supported square plates. We retain the reduced integration technique that was successfully applied in [Carrera and DeMasi 2002b]. LW as well as ESL analyses have been performed for Q4, Q8 and Q9 elements.

We consider four-layer plates, with the two inner layers consisting of cross-ply [0°/90°] carbon fiber and the external skins made of piezoceramic material PZT-4. The material properties are shown in Table 2 on page 432. The two composite layers have thickness $h_2 = h_3 = 0.4h$ and the skins have $h_1 = h_4 = 0.1h$. The unit value is assigned to the plate thickness. A bisinusoidal distribution of transversal pressure with amplitude $\hat{p}_z = 1$ is applied to the top surface (this coincides with a sensor configuration case).

Figure 2 shows the in-plane displacement u_y distribution in the thickness direction for the selected plate elements (z is the horizontal axis). Better results are obtained for the LFM and EFMZC analyses with respect to ones based on P-RMVT. The number of elements for the plate side N_e has been placed to the right of the acronym. Layerwise analysis leads to much better results than ESL.

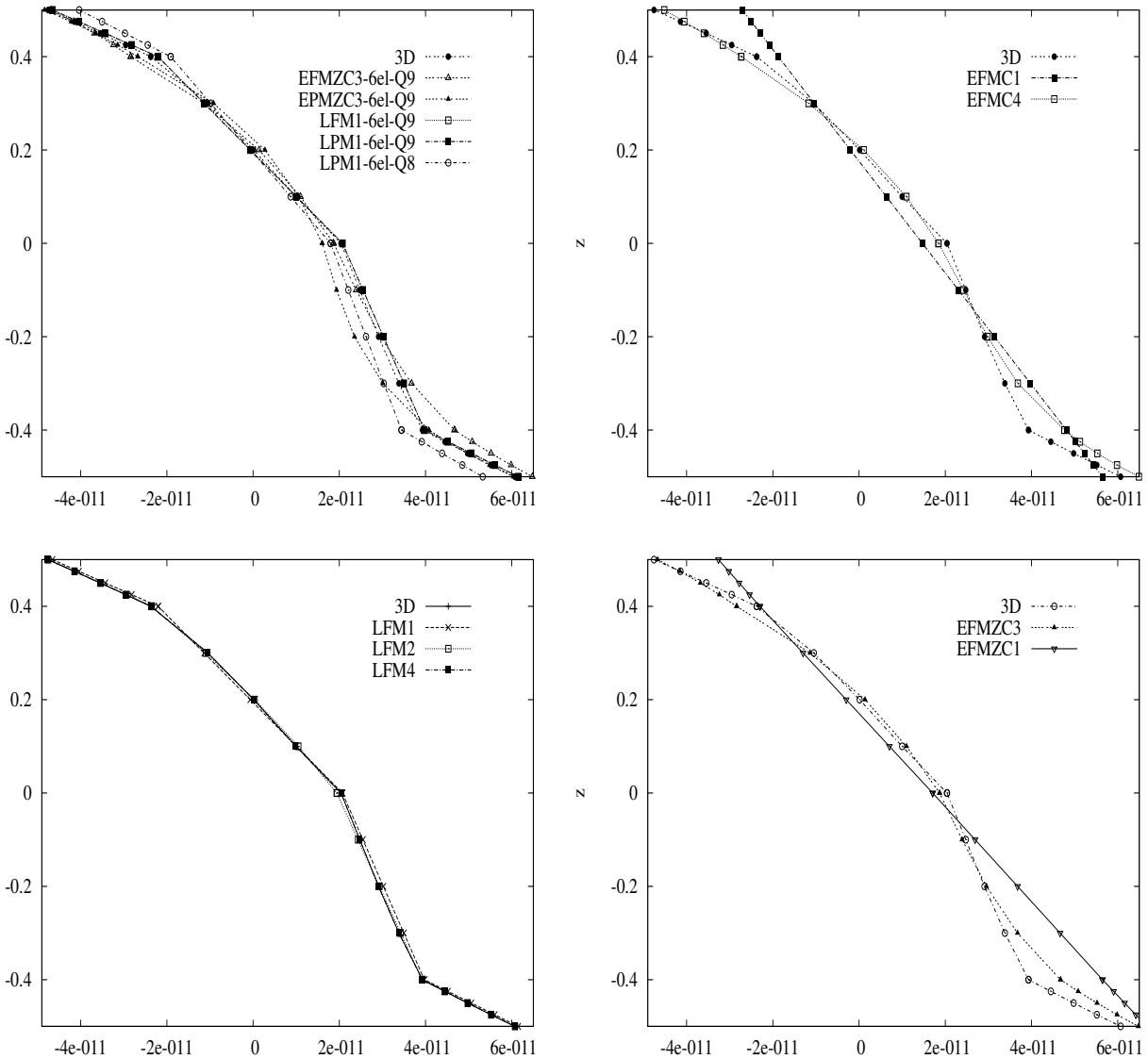

Figure 2. Performance of various FEs in predicting the displacement $u_y(a/2, 0)$ versus z. The a/h ratio equals 4. Curves labeled "3D" show the exact solution reported in [Heyliger 1994]; the remaining curves show the results obtained from FE approaches based on F-RMVT and P-RMVT (upper left), ESL theory (upper right); LW theory (lower left), and ESL theory incorporating Murakami's zigzag function (lower right).

Property	PZT-4	Gr/Ep	PVDF	Property	PZT-4	Gr/Ep	PVDF
E_1 (GPa)	81.3	132.38	236.99	e_{15} (C/m^2)	12.72	0	−0.01
E_2 (GPa)	81.3	10.756	23.19	e_{24} (C/m^2)	12.72	0	−0.01
E_3 (GPa)	64.5	10.756	10.43	e_{31} (C/m^2)	−5.20	0	−0.13
ν_{12}	0.329	0.24	0.1541	e_{32} (C/m^2)	−5.20	0	−0.14
ν_{13}	0.432	0.24	0.1787	e_{33} (C/m^2)	15.08	0	−0.28
ν_{23}	0.432	0.49	0.1780	ϵ_{11}/ϵ_0	1475	3.5	12.50
G_{23} (GPa)	25.6	3.606	2.15	ϵ_{22}/ϵ_0	1475	3.0	11.98
G_{13} (GPa)	25.6	5.6537	4.4	ϵ_{33}/ϵ_0	1300	3.0	11.98
G_{12} (GPa)	30.6	5.6537	6.43	ρ	1	1	1

Table 2. Mechanical and electrical material properties.

The same conclusions can be drawn for the transversal normal stress evaluation in Figure 3. The use of LW elements with at least a parabolic distribution ($N = 2$) in each layer is required. Remarkable improvements are obtained when the Murakami zigzag function is used.

Data related to the transversal electrical displacement $\mathcal{D}_z$, shown in Figure 4, are of particular interest. Various numbers of nodes for elements and FE meshes are compared (top left). There are difficulties when certain FEs are used to predict $\mathcal{D}_z$ in the piezoelectric layers (top right pane of figure); the results' accuracy is very much dependent on the choice of a model, and the use of elements of type LM2 (at least) appears to be necessary for correct predictions. This suggests that the use of F-RMVT may be mandatory for the accurate computation of *interlaminar continuous* $\mathcal{D}_z$ at a reasonable computational cost, and that

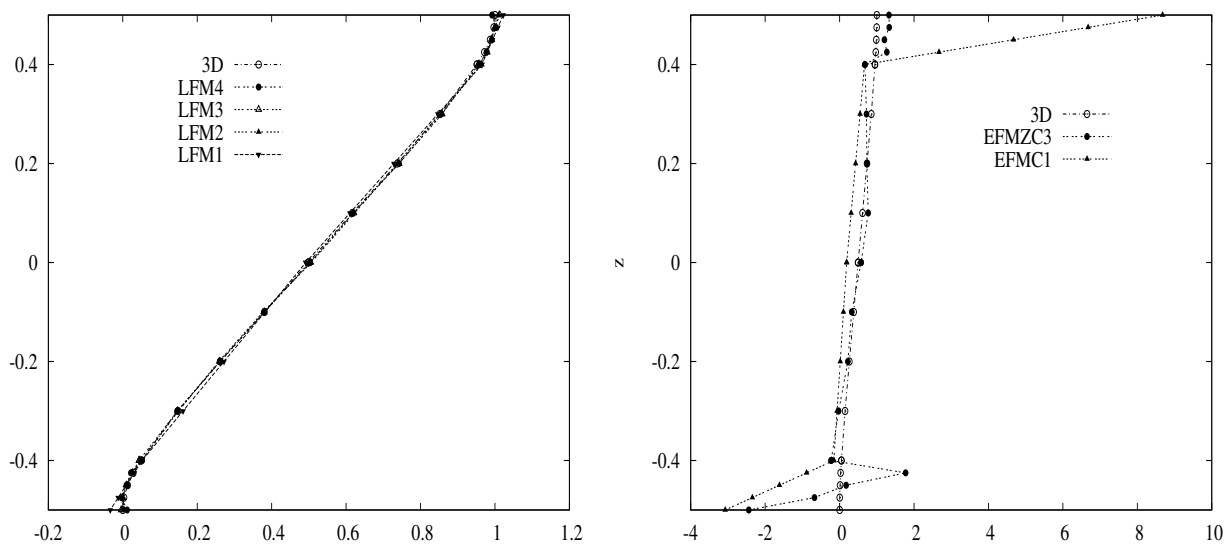

Figure 3. Performance of various FEs in predicting the transverse normal stress $\sigma_{zz}(a/2, b/2)$ versus z. The ratio a/h equals 4.

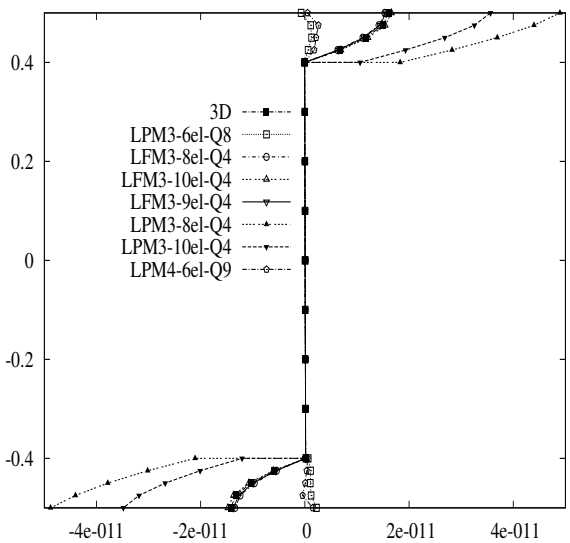

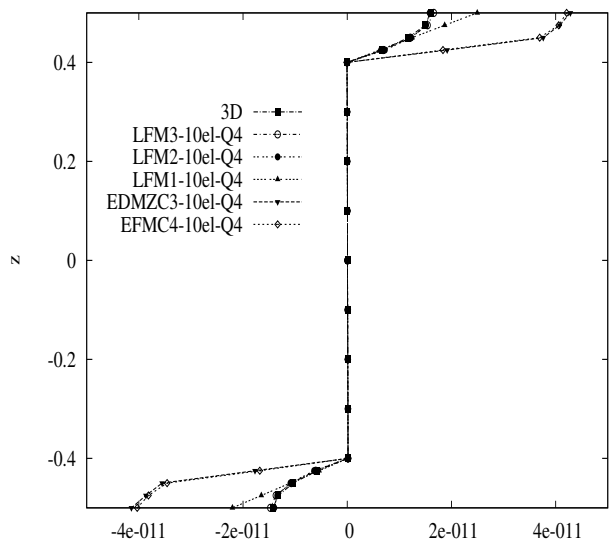

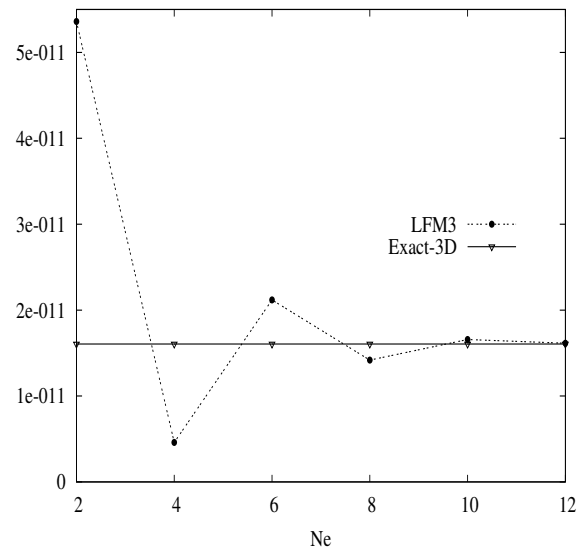

a/h	2	4	10
3D [Heyliger 1994]	/	160.58	/
LFM4	261.73	161.50	137.55
LPM4	316.30	301.4	941.94
LD4	284.94	212.66	439.78
LFM3	263.79	161.89	137.70
LPM3	306.17	299.41	942.06
LD3	286.90	213.17	417.54
LFM2	254.67	153.87	130.17
LPM2	310.83	290.39	923.49
LD2	300.96	223.83	430.72
EFMZC3	549.81	371.98	350.39
EFMC4	516.85	357.11	346.49

Figure 4. Top: performance of various FEs in predicting the transverse electric displacement $\mathcal{D}_z(a/2, b/2)$ versus z, with $a/h = 4$. (Left: LW elements with various number of nodes per element; right: LW and ESL elements for the Q4 case.) Bottom left: Convergence analysis for Q4 elements. Bottom right: Dependence of $\mathcal{D}_z(a/2, b/2, h) \times 10^{13}$ on the ratio a/h, for a $[12 \times 12]$ mesh and Q4 element.

P-RMVT and ESL results may be unacceptable. (Since the electric charge Q over a piezoelectric patch is obtained by integrating the $\mathcal{D}_z$ distribution over the patch's surface, wrong $\mathcal{D}_z$ values lead to wrong Q values, potentially rendering the closed-loop control completely meaningless.)

Note that the accuracy obtainable with LFM2 is comparable with what we get with LPM4, confirming that the use of P-RMVT is advantageous as far as computational effort is concerned. For the sake of

completeness, Figure 4 shows the convergence rate of the Q4 elements; they are consistent with those found for of pure mechanical problems in our earlier work. Various plate thickness ratio values are considered in the table at the bottom right of Figure 4, showing the importance of UF as a tool to establish an assessment of simplified, classical and advanced FEs for piezoelectric plate analysis.

These results are confirmed in the evaluation of the electrical voltage distribution versus, shown in Figure 5. The largest discrepancies among the theories are experienced in the evaluation of electrical displacements.

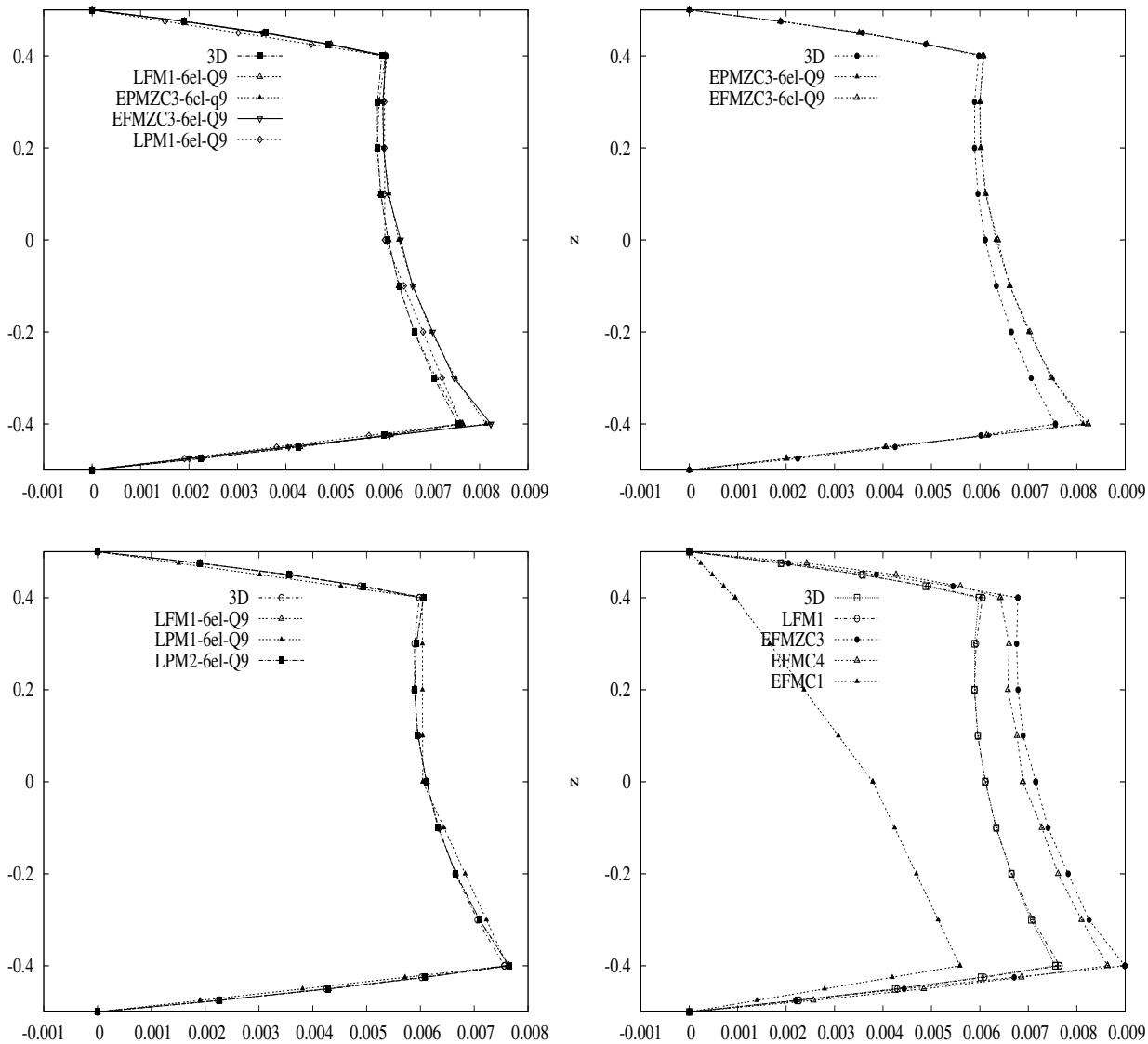

Figure 5. Top: performance of various FEs in predicting the transverse electric potential $\Phi(a/2, b/2)$ versus z, with $a/h = 4$, a $[6 \times 6]$ mesh and a Q9 element.

a/h	2	4	10	a/h	2	4	10
exact 3D	/	30,03	/	LFM1	4.751	30.13	587.4
LFM4	4.949	30.27	587.1	LPM1	4.761	30.16	587.8
LPM4	4.947	30.27	587.1	EFMZC3	4.731	31.11	623.4
LD4	4.909	30.03	582.2	EPMZC3	4.487	28.91	579.3
LFM3	4.953	30.27	587.1	EFMZC2	4.719	24.55	566.2
LPM3	4.952	30.27	587.1	EPMZC2	2.881	21.26	529.5
LD3	4.909	30.03	582.2	EFMC4	5.224	31.66	623.6
LFM2	4.928	30.23	586.9	EPMC4	5.564	28.97	579.4
LPM2	4.928	30.23	587.0	EFMC3	4.956	30.95	621.2
LD2	4.894	29.98	581.9	EPMC3	4.713	28.96	578.2

Table 3. Evaluation of $u_z(a/2, b/2, 0) \times 10^{11}$; mesh $[6 \times 6]$ and Q9 elements. The exact 3D data are taken from [Heyliger 1994].

Table 3 compares our results, for both mechanical and electrical variables, with the three-dimensional exact solution and the results of Garcia Lage et al. [2004b]. A square plate is considered with a lay-up [0°/90°/0] for the internal layers; two piezoelectric layers of PVDF materials (see Table 2) are used as external skins. As in this last reference, the peak value of the applied pressure is 3 Pa. The relative errors are displayed in Table 4. The superiority of the full implementation of RMVT is still remarkable.

7. Concluding remarks

The paper extends the Unified Formulation and the Reissner Mixed Variational Theorem to the development of finite elements for the static analysis of piezoelectric plates with *a priori* continuous transverse electrical displacement components $\mathcal{D}_z$. The following main conclusions can be drawn.

(1) It has been confirmed that UF is a valuable tool in the hierarchical analysis of piezoelectric plates using the finite element method. The implemented FEs, in fact, can provide very accurate descriptions of both mechanical and electrical fields.

(2) FEs with interlaminar continuous $\mathcal{D}_z$ appear to be very suitable for piezoelectric plate analysis. Better results are obtained with respect to the other FEs herein compared.

(3) In order to preserve computational efforts, the use of the proposed elements would seem to be mandatory if accurate evaluations of $\mathcal{D}_z$ and the related electric charge are required.

Future developments should be directed towards considering the analysis of piezoelectric plate with localized patches as sensors and/or actuators. Other plate lay-ups and the effect of additional boundary conditions and geometries should be examined. The case of imposed $\mathcal{D}_z$ at the interface should in particular be analyzed.

References

[Auricchio et al. 2001] F. Auricchio, P. Bisegna, and C. Lovadina, "Finite element approximation of piezoelectric plates", *Int. J. Numer. Methods Eng.* **50**:6 (2001), 1469–1499.

	$\sigma_{zz}(a/2, b/2, 0.5)$ [Pa]	$\sigma_{yz}(a/2, 0, 0)$ [Pa]	$\sigma_{xx}(a/2, b/2, 0.5)$ [Pa]
Exact 3D	3.000	2.614	33.71
LFM4	3.0043 (0.14%)	2.6239 (0.37%)	34.54 (2.46%)
LPM4	3.0063 (0.21%)	2.6486 (1.32%)	34.54 (2.46%)
LD4	3.0081 (0.27%)	2.7302 (4.44%)	34.50 (2.34%)
Literature	3.022 (0.73%)	2.610(−0.16%)	33.08 (−1.87%)
	$\mathcal{D}_z(a/2, b/2, 0.5)\times 10^{11}$ [C/m^2]	$\Phi(a/2, b/2, 0)\times 10^{3}$ [V]	$\sigma_{yy}(a/2, b/2, 0.166^{+})$ [Pa]
Exact 3D	−4.970	1.28	−19.63
LFM4	−5.0234 (1.07%)	1.2835 (0.27%)	−19.41 (−1.12%)
LPM4	−5.0456 (1.52%)	1.2834 (0.26%)	−19.39 (−1.22%)
LD4	−5.0509 (1.62%)	1.2837 (0.28%)	−19.41 (−1.12%)
Literature	−4.998 (0.56%)	1.279(−0.07%)	−19.46 (−0.87%)
	$u_z(a/2, b/2, 0.5)\times 10^{11}$ [m]	$u_x(0, b/2, 0.5)\times 10^{12}$ [m]	$u_y(a/2, 0, 0.5)\times 10^{12}$ [m]
Exact 3D	1.529	−1.719	−3.507
LFM4	1.5394 (0.68%)	−1.719 (0.0%)	−3.5045 (−0.07%)
LPM4	1.5395 (0.68%)	−1.7203 (0.075%)	−3.5053 (−0.048%)
LD4	1.5276 (−0.091%)	−1.7224 (0.075%)	−3.5046 (−0.068%)
Literature	1.532 (0.19%)	−1.675 (−2.56%)	−3.475 (−0.90%)

Table 4. Comparison of present analysis with respect to available results: mesh $[6\times 6]$, $a/h = 4$, Q8 element ($^{+}$ means top value). The literature values are from [Garcia Lage et al. 2004b]

[Ballhause et al. 2005] D. Ballhause, M. D'Ottavio, B. Kröplin, and E. Carrera, "A unified formulation to assess multilayered theories for piezoelectric plates", *Comput. Struct.* **83**:15-16 (2005), 1217–1235.

[Batra and Vidoli 2002] R. C. Batra and S. Vidoli, "Higher-order piezoelectric plate theory derived from a three-dimensional variational principle", *AIAA J.* **40**:1 (2002), 91–104.

[Benjeddou 2000] A. Benjeddou, "Advances in piezoelectric finite element modeling of adaptive structural elements: a survey", *Comput. Struct.* **76**:1-3 (2000), 347–363.

[Carrera 1995] E. Carrera, "A class of two dimensional theories for multilayered plates analysis", *Mem. Accad. Sci. Torino Cl. Sci. Fis. Mat. Natur.* **19-20** (1995), 49–87.

[Carrera 1996] E. Carrera, "C^0 Reissner–Mindlin multilayered plate elements including zig-zag and interlaminar stresses continuity", *Int. J. Numer. Methods Eng.* **39**:11 (1996), 1797–1820.

[Carrera 1997] E. Carrera, "An improved Reissner–Mindlin type element for the electromechanical analysis of multilayered plates including piezo layers", *J. Intell. Mater. Syst. Struct.* **8**:3 (1997), 232–248.

[Carrera 1999a] E. Carrera, "A Reissner's mixed variational theorem applied to vibrational analysis of multilayered shell", *J. Appl. Mech. (ASME)* **66**:1 (1999), 69–78.

[Carrera 1999b] E. Carrera, "A study of transverse normal stress effects on vibration of multilayered plates and shells", *J. Sound Vib.* **225**:5 (1999), 803–829.

[Carrera 2001] E. Carrera, "Developments, ideas, and evaluations based upon Reissner's mixed variational theorem in the modeling of multilayered plates and shells", *Appl. Mech. Rev.* **54**:4 (2001), 301–329.

[Carrera 2003a] E. Carrera, "Historical review of zig-zag theories for multilayered plates and shell", *Appl. Mech. Rev.* **56**:3 (2003), 287–308.

[Carrera 2003b] E. Carrera, "Theories and finite elements for multilayered plates and shells: a unified compact formulation with numerical assessment and benchmarking", *Arch. Comput. Methods Eng.* **10**:3 (2003), 215–296. Zbl 02097772

[Carrera and Boscolo 2006] E. Carrera and M. Boscolo, "Classical and mixed finite elements for static and dynamics analysis of piezoelectric plates", *Int. J. Numer. Methods Eng.* (2006). Published online 6 Nov 2006.

[Carrera and DeMasi 2002a] E. Carrera and L. DeMasi, "Classical and advanced multilayered plate elements based upon PVD and RMVT, 1: Derivation of finite element matrices", *Int. J. Numer. Methods Eng.* **55**:2 (2002), 191–231.

[Carrera and DeMasi 2002b] E. Carrera and L. DeMasi, "Classical and advanced multilayered plate elements based upon PVD and RMVT, 2: Numerical implementations", *Int. J. Numer. Methods Eng.* **55**:3 (2002), 253–291.

[Carrera et al. 2005] E. Carrera, S. Brischetto, and M. D'Ottavio, "Vibrations of piezoelectric shells by unified formulations in the Reissner's mixed theorem", in *SMART '05: Second ECCOMAS Thematic Conference on Smart Structures and Materials* (Lisbon), edited by C. A. Mota Soares et al., 2005.

[Chopra 1996] I. Chopra, "Review of current status of smart structures and integrated systems", pp. 20–62 in *Smart structures and materials 1996: Smart structures and integrated systems* (San Diego, CA), edited by I. Chopra, Proceedings of SPIE **2717**, SPIE, Bellingham, WA, 1996.

[Chopra 2002] I. Chopra, "Review of state of art of smart structures and integrated systems", *AIAA J.* **40**:11 (2002), 2145–2187.

[Crawley and de Luis 1987] E. F. Crawley and J. de Luis, "Use of piezoelectric actuators as elements of intelligent structures", *AIAA J.* **25**:10 (1987), 1373–1385.

[D'Ottavio and Kröplin 2006] M. D'Ottavio and B. Kröplin, "An extension of Reissner mixed variational theorem to piezoelectric laminates", *Mech. Adv. Mater. Struct.* **13**:2 (2006), 139–150.

[Garcia Lage et al. 2004a] R. Garcia Lage, C. M. Mota Soares, C. A. Mota Soares, and J. N. Reddy, "Layerwise partial mixed finite element analysis of magneto-electro-elastic plates", *Comput. Struct.* **82**:17-19 (2004), 1293–1301.

[Garcia Lage et al. 2004b] R. Garcia Lage, C. M. Mota Soares, C. A. Mota Soares, and J. N. Reddy, "Modeling of piezolaminated plates using layer-wise mixed finite elements", *Comput. Struct.* **82**:23-26 (2004), 1849–1863.

[Heyliger 1994] P. Heyliger, "Static behavior of laminated elastic/piezoelectric plates", *AIAA J.* **32**:12 (1994), 2481–2484.

[Heyliger and Saravanos 1995] P. Heyliger and D. A. Saravanos, "Exact free-vibration analysis of laminated plates with embeded piezoelectric layers", *J. Acoust. Soc. Am.* **98**:3 (1995), 1547–1557.

[Ikeda 1996] T. Ikeda, *Fundamentals of piezoelectricity*, corrected ed., Oxford University Press, New York, 1996.

[Kögl and Bucalem 2005a] M. Kögl and M. L. Bucalem, "Analysis of smart laminates using piezoelectric MITC plate and shell elements", *Comput. Struct.* **83**:15-16 (2005), 1153–1163.

[Kögl and Bucalem 2005b] M. Kögl and M. L. Bucalem, "A family of piezoelectric MITC plate elements", *Comput. Struct.* **83**:15-16 (2005), 1277–1297.

[Lee 1990] C. K. Lee, "Theory of laminated piezolectric plates for the design of distributed sensors/actuators, I: Governing equations and reciprocal relationships", *J. Acoust. Soc. Am.* **87**:3 (1990), 1144–1158.

[Mitchell and Reddy 1995] J. A. Mitchell and J. N. Reddy, "High frequency vibrations of piezoelectric cristal plates", *Int. J. Solids Struct.* **32**:16 (1995), 2345–2367.

[Oh and Cho 2004] J. Oh and M. Cho, "A finite element based on cubic zig-zag plate theory for the prediction of thermo-electric-mechanical behaviors", *Int. J. Solids Struct.* **41**:5-6 (2004), 1357–1375. In press.

[Reissner 1984] E. Reissner, "On a certain mixed variational theory and a proposed application", *Int. J. Numer. Methods Eng.* **20**:7 (1984), 1366–1368.

[Robbins and Reddy 1991] D. H. Robbins and J. N. Reddy, "Analysis of piezoelectric actuated beams using a layer-wise displacements theory", *Comput. Struct.* **41**:2 (1991), 265–279.

[Saravanos and Heyliger 1999] D. A. Saravanos and P. R. Heyliger, "Mechanics and computational models for laminated piezoelectric beams, plates, and shells", *Appl. Mech. Rev.* **52**:10 (1999), 305–320.

[Sheikh et al. 2001] A. H. Sheikh, P. Topdar, and S. Halder, "An appropriate fe model for through-thickness variation of displacement and potential in thin moderately thick smart laminates", *Compos. Struct.* **51**:4 (2001), 401–409.

[Shu 2005] X. Shu, "Free-vibration of laminated piezoelectric composite plates based on an accurate theory", *Compos. Struct.* **67**:4 (2005), 375–382.

[Thornbuegh and Chattopadhyay 2002] R. P. Thornbuegh and A. Chattopadhyay, "Simultaneous modeling of mechanical and electrical response of smart composite structures", *AIAA J.* **40**:8 (2002), 1603–1610.

[Tiersten 1969] H. F. Tiersten, *Linear piezoelectric plate vibrations*, Plenum Press, New York, 1969.

[Vidoli and Batra 2000] S. Vidoli and R. C. Batra, "Derivation of plate and rod equations for a piezolectric body from a mixed three-dimensional variational principle", *J. Elasticity* **59**:1-3 (2000), 23–50.

[Wang and Yang 2000] J. Wang and J. Yang, "High-order theories of piezoelectric plates and applications", *Appl. Mech. Rev.* **53**:4 (2000), 87–96.

[Wang et al. 1997] J. Wang, Y.-K. Yong, and T. Imai, "Finite element analysis of the piezoelectric vibrations of quartz plate resonators with higher-order plate theory", pp. 650–658 in *Proceedings of the 1997 IEEE International Frequency Control Symposium* (Orlando, FL), IEEE, New York, 1997.

[Yang and Batra 1995] J. S. Yang and R. C. Batra, "Mixed variational principles in non-linear electroelasticity", *Int. J. Non-Linear Mech.* **30**:5 (1995), 719–725.

Received 9 Oct 2006. Accepted 29 Nov 2006.

ERASMO CARRERA: erasmo.carrera@polito.it
Dept. of Aeronautics and Aerospace Engineering, Politecnico di Torino, Corso Duca degli Abruzzi, 24, 10129 Torino, Italy

CHRISTIAN FAGIANO: C.Fagiano@tudelft.nl
Dept. of Aeronautics and Aerospace Engineering, Politecnico di Torino, Corso Duca degli Abruzzi, 24, 10129 Torino, Italy
Current address: *Department of Mechanics, Aerospace Structures and Materials, Delft University of Technology, P.O. Box 5058, 2600 GB Delft, Netherlands*